Magnetic anisotropy of titanomagnetites $Fe_{3-x}Ti_xO_4$, $0 \leq x \leq 0.55$

Z. Kąkol*
Department of Chemistry, Purdue University, West Lafayette, Indiana 47907

J. Sabol
Department of Chemistry, Ohio Northern University, Ada, Ohio 45810

J. M. Honig
Department of Chemistry, Purdue University, West Lafayette, Indiana 47907
(Received 14 December 1990)

Magnetization measurements reported for $Fe_{3-x}Ti_xO_4$ in the composition range $0 \leq x \leq 0.55$ were used to determine the magnetic-anisotropy coefficients as a function of x and of temperature. Magnetic measurements were performed along the principal crystallographic directions in applied fields up to 15 kOe and in the temperature range 4.2 to 300 K on single-crystalline specimens that had been annealed so as to preserve the ideal oxygen stoichiometry. Magnetic-anisotropy parameters were calculated from magnetization curves and analyzed in terms of estimated magnetoelastic contributions to the magnetic anisotropy, with use of published magnetostriction and elastic-constant data. The anisotropy constant K_1 passes through a minimum at $x = 0.2$, irrespective of temperature, at a composition where Fe^{2+} first begins to appear in tetrahedral interstitial sites; K_1 grows rapidly with increasing x for $x > 0.2$. The results show that the magnetoelastic contribution to the magnetic anisotropy dominates at high x and originates from the presence of Fe^{2+} Jahn-Teller ions on the tetrahedral sublattice. Within the large theoretical uncertainties, the variation of K_1 with temperature could be adequately reproduced by the theory.

INTRODUCTION

The magnetic and crystallographic properties of the titanomagnetite (TM) series $Fe_{3-x}Ti_xO_4$ change significantly over the compositional range $0 \leq x \leq 1$. Despite the fact that these variations are of interest to both the commercial sector and the physics, chemistry, and geoscience communities, very little work has been published in this area. Large magnetostriction and magnetic anisotropy effects were reported by Syono and Ishikawa[1] for samples with $x > 0.5$ at low temperatures. The remanent magnetization and coercive force in polycrystalline specimens were reported by Banerjee *et al.*[2] to rise rapidly with increasing $x(>0.5)$ at 77 K. These findings were later confirmed by Schmidbauer and Readman[3] and in measurements on single crystals by Kąkol *et al.*[4] There also have been some earlier investigations of the elastic and magnetic properties[5–8] of ulvöspinel (US): technically, this material is assigned the formula Fe_2TiO_4, but compositions $Fe_{3-x}Ti_xO_4$ with $x > 0.96$ are unstable. In the above reports Ishikawa, Syono, and their coworkers demonstrated that the physical properties of US differ greatly from those of Fe_3O_4 and other ferrites: (i) US exhibits a large tetragonal distortion, which at 77 K attains a value of $(c-a)/a = 7.5 \times 10^{-3}$, a and c being the lattice parameters; this distortion is magnetostrictive in origin because it is encountered only below the Curie temperature T_C and because the direction of elongation can be switched by application of an external magnetic field. (ii) The elastic constants $(C_{11}\text{-}C_{12})$ are roughly one order of magnitude smaller in US, as compared to Fe_3O_4, over the temperature range 77–300 K. This reduction is attributed to the Jahn-Teller (JT) effect arising from the presence of the Fe^{2+} ions on the tetrahedral interstices of the US, denoted hereafter as $(Fe^{2+})_t$—in contrast to $(Fe^{2+})_o$ for octahedrally coordinated ferrous ions. The difference $C_{11}\text{-}C_{12}$ diminishes with temperature for T well above T_c, suggesting[9,10] that lattice softening arises from Jahn-Teller distortions. The above anomalies in US were explained by Kataoka[11] in terms of a model which considers the interference between the JT effect correlated to with $(Fe^{2+})_t$ ions and the spin-lattice coupling effects which involve the $(Fe^{2+})_o$ species.

In light of the above developments it seemed of interest to study the magnetic properties of the TM series in the composition range intermediate between Fe_3O_4 and US. In particular, one can expect considerable changes in properties that depend on the $[Fe^{2+}]/[Fe^{3+}]$ ratio, which varies dramatically with x for cations located both on t and on o sites. Several types of Fe^{2+}-Fe^{3+} cation distributions have been proposed.[4,12–15] As is well established,[16] Ti^{4+} is located exclusively on o interstices, with concomitant alterations in the Fe^{2+} and Fe^{3+} concentration on both types of sublattices. In Fig. 1 we show the most recently proposed cation distribution,[4] based on saturation magnetization measurements carried out on single crystals.

In this paper we report on the magnetic anisotropy of the TM series $Fe_{3-x}Ti_xO_4$ over a wide range of x and T, and we interpret the findings in terms of the observed large magnetostriction. A preliminary report on this subject has been published.[17]

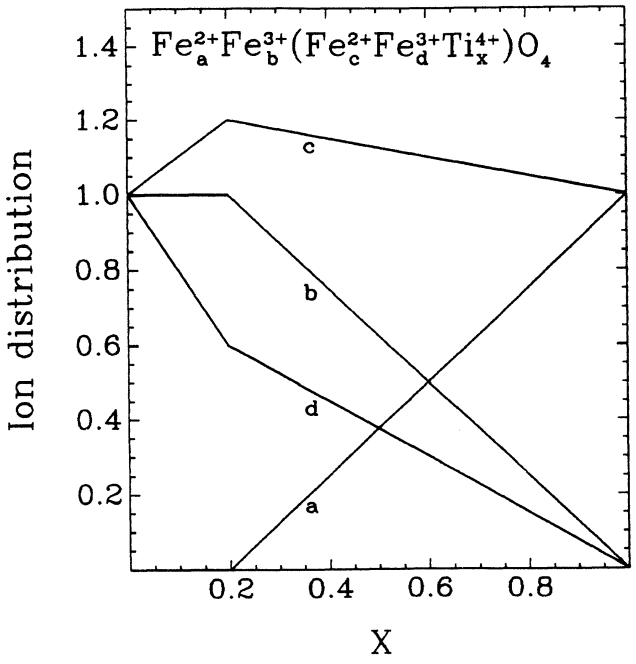

FIG. 1. Ion distribution in the $Fe_{3-x}Ti_xO_4$ series vs compositional parameter x.

EXPERIMENTAL

Single crystals of $Fe_{3-x}Ti_xO_4$ $(0<x<0.95)$ were grown by a cold crucible skull-melting technique that has been described elsewhere in detail.[18] The advantage of this method is that no impurities are introduced during crystal growth. In postannealing procedures[19] the ideal oxygen to metal ratio of 4:3 was established for each crystal by heating for 36–48 h in appropriate CO and CO_2 atmospheres at 1400 °C.[20,21] The uncertainty in oxygen stoichiometry is estimated to be ±0.0001. The samples were rapidly quenched and ground into spheres of 1–2 mm diameter. Their uniformity in composition was checked using a microprobe electron analyzer. The uncertainty in x is estimated to be ±0.001. Laue back reflection x-ray photography was used to orient the crystals.

Magnetic measurements along the principal crystallographic directions were performed on a vibrating sample magnetometer in applied fields up to 15 kOe and in the temperature range 4.2–300 K. The instrument was calibrated against several magnetic standards: Ni, Er_2O_3, and $HgCo(SCN)_4$.

DATA AND CALCULATIONS

In Figs. 2 and 3 we display magnetization curves in applied magnetic fields H_a and their dependence on temperature, composition, and crystallographic direction. These measurements are representative of a broader study; see Ref. 22 for additional data. The temperature dependence of the saturation magnetization M_s for the $Fe_{3-x}Ti_xO_4$ series with $x \leq 0.55$ is displayed in Fig. 4.

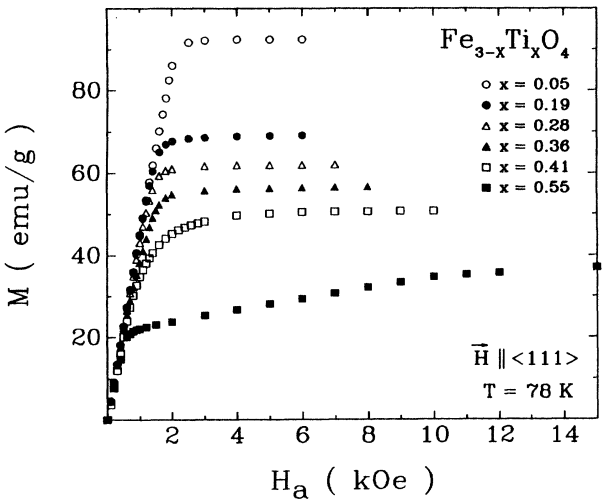

FIG. 2. Magnetization curves of $Fe_{3-x}Ti_xO_4$ series along ⟨111⟩ direction at 78 K.

These fundamental data, which are of intrinsic interest, form the basis of the subsequent theoretical analysis.

The magnetic anisotropy effects are conventionally analyzed in terms of the expression

$$E_A = K_1(\alpha_1^2\alpha_2^2+\alpha_2^2\alpha_3^2+\alpha_3^2\alpha_1^2)+K_2(\alpha_1^2\alpha_2^2\alpha_3^2)+\cdots \quad (1)$$

for the anisotropy energy E_A of cubic crystals. Here K_1 and K_2 are the anisotropy coefficients and α_i are the direction cosines of the magnetization vector with respect

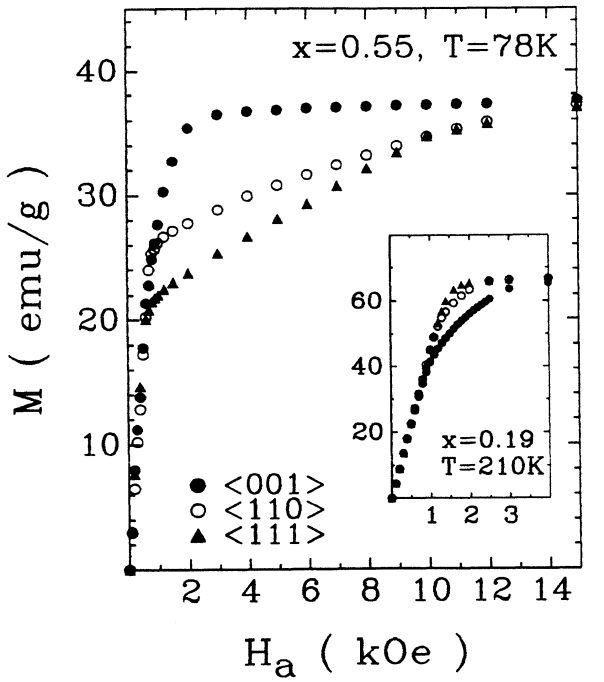

FIG. 3. Magnetization curves along ⟨001⟩, ⟨110⟩, and ⟨111⟩ directions for $Fe_{2.45}Ti_{0.55}O_4$ at 78 K (maximum positive K_1) and for $Fe_{2.81}Ti_{0.19}O_4$ at 210 K (maximum negative K_1).

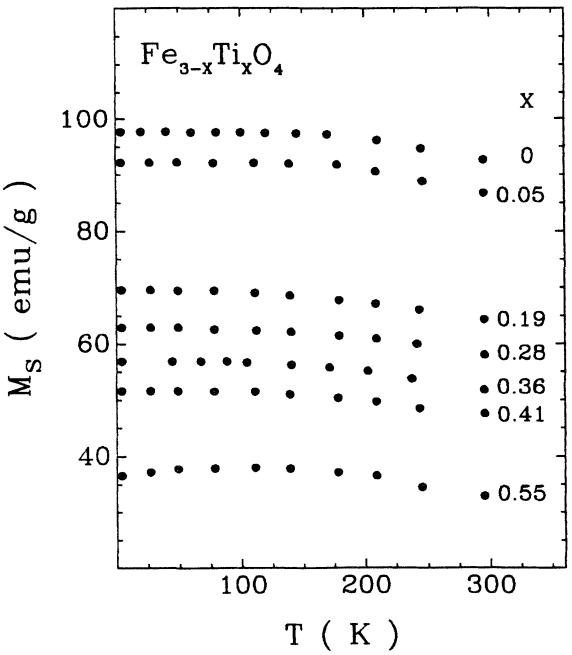

FIG. 4. Temperature dependence of the saturation magnetization for the $Fe_{3-x}Ti_xO_4$ series.

to the cubic axes of the crystal.

We determined the anisotropy coefficients by calculating the energy required to saturate the specimen magnetically along different directions. The magnetization energy density is found from the relation

$$W=\int_0^{M_s} H_a dM \ , \tag{2}$$

which can be calculated from the area between the ordinate and the $M(H_a)$ curve. This energy density is equal to the change in anisotropy energy for the magnetization process. For cubic crystals one may show that

$$K_1=4(W_{[110]}-W_{[001]}) \ , \tag{3}$$

$$K_2=9\{3(W_{[111]}-W_{[001]})-4(W_{[110]}-W_{[001]})\} \ , \tag{4}$$

where the W subscripts designate the directions along which the magnetization measurements are executed.

The above methodology fails when hysteresis effects interfere with the measurements. These effects became prominent at low temperatures for $x>0.55$. Thus, K_1 and K_2, as determined above, are subject to considerable experimental error. Therefore, a more elaborate procedure is required, in which the anisotropy parameters determined by (3) and (4) serve as inputs. The method involves the direct calculation of $M(H_a)$ through a self-consistent numerical procedure in applied fields greater than those needed to eliminate domain wall motion. The rotation of the domain magnetization against the magnetic anisotropy forces then becomes the dominant mechanism of the magnetization process.

The total energy change E accompanying the magnetization is now given by

$$E=E_A-M_sH_{\text{eff}}, \quad H_{\text{eff}}=H_a-H_d \ , \tag{5}$$

where H_{eff} is the effective magnetic field and H_d is the demagnetization field $H_d=NM$, with N representing the demagnetization factor, calculated from the initial slope of the M versus H curve (see Fig. 3).

Let θ and ϕ represent, respectively, the angle between M and the [001] axis direction, and between the projection of M_s onto the (001) plane and the [100] axis. Then, according to Eqs. (1) and (5) we find

$$E=K_1\sin^2\theta(\sin^2\theta\cos^2\phi\sin^2\phi+\cos^2\theta)+K_2(\sin^4\theta\cos^2\theta\sin^2\phi\cos^2\phi)$$
$$-M_sH_a(\beta_x\sin\theta\cos\phi+\beta_y\sin\theta\sin\phi+\beta_z\cos\theta)+NM_s^2 \ , \tag{6}$$

where β_j are the direction cosines of the applied field. On introducing the equilibrium constraints

$$\partial E/\partial\theta=0 \quad \text{and} \quad \partial E/\partial\phi=0 \tag{7}$$

one obtains two equations that can be solved for θ and ϕ once M_s, H_a, N, and initial trial values for K_1 and K_2 are inserted. From θ and ϕ the orientation of the magnetization vector is established; M can now be calculated for a series of H_a values so that the resultant curve can be compared with experiment in the range where domain wall motion no longer occurs. A new trial set of K_1 and K_2 is then introduced and the procedure is continued until the best fit to the experimental data is obtained.

The general procedure outlined above can be considerably simplified if H_a is directed along the high symmetry axes of the crystal. For example, if the magnetization for a specimen with positive K_1 (easy axis parallel to $\langle 001\rangle$) is generated by a magnetic field applied along a [110] direction then the domains remaining after the wall displacement is completed are reduced to [100] and [010] domains. The subsequent magnetization involves the rotation of domain magnetization in the (001) plane. Condition (7) as applied to (6) now leads to the simple result

$$2\left[\frac{M}{M_s}\right]^3-\frac{M}{M_s}=\frac{H_aM_s}{2K_1} \ , \tag{8}$$

which permits K_1 to be readily found.

An illustration of the above procedure is furnished in Fig. 5 where we compare the calculated $M(H_a)$ curve to the experimental measurements on $Fe_{2.45}Ti_{0.55}O_4$ at several temperatures. The agreement is seen to be satisfactory.

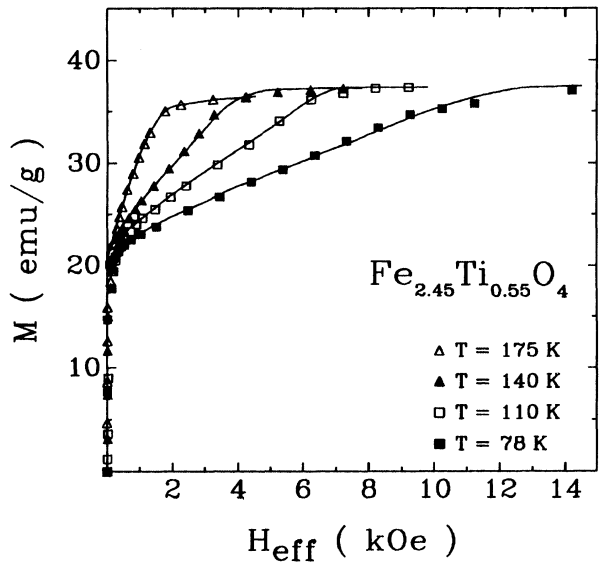

FIG. 5. Calculated magnetization curves of $Fe_{2.45}Ti_{0.55}O_4$ at selected temperatures. Experimental data are entered as points.

RESULTS

The K_1 anisotropy coefficients as calculated by the above procedures are entered in Fig. 6 to show their dependence on sample composition x at a selected set of temperatures. The temperature dependence of K_1 for selected titanomagnetites is displayed in Figs. 7(a) and 7(b). The insets show comparable variations in K_2.

The following features are noteworthy. (i) At all temperatures the anisotropy constant K_1 passes through a minimum (the maximum anisotropy field along the $\langle 100 \rangle$ direction) for a Ti concentration of $x \approx 0.2$. This coincides with the point beyond which Fe^{2+} is first forced onto tetrahedral sites with rising concentrations of Ti; see Fig. 1. After an initial drop to the minimum value, K_1 rises with an increasing $(Fe^{2+})_t$ content. (ii) Also, beyond $x=0.2$ the variation of K_1 with temperature is much more marked than for samples with low Ti content. Furthermore, this trend results in a change of

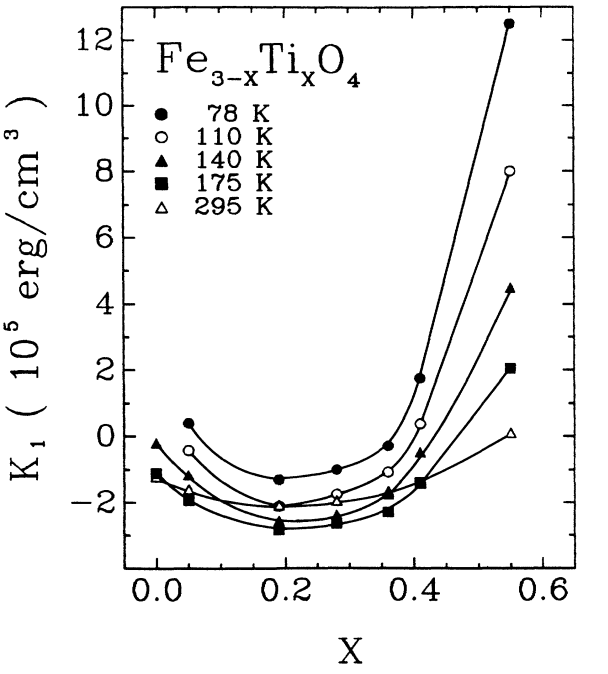

FIG. 6. Anisotropy parameter K_1 vs x for $Fe_{3-x}Ti_xO_4$ at selected temperatures in the 78–295 K range.

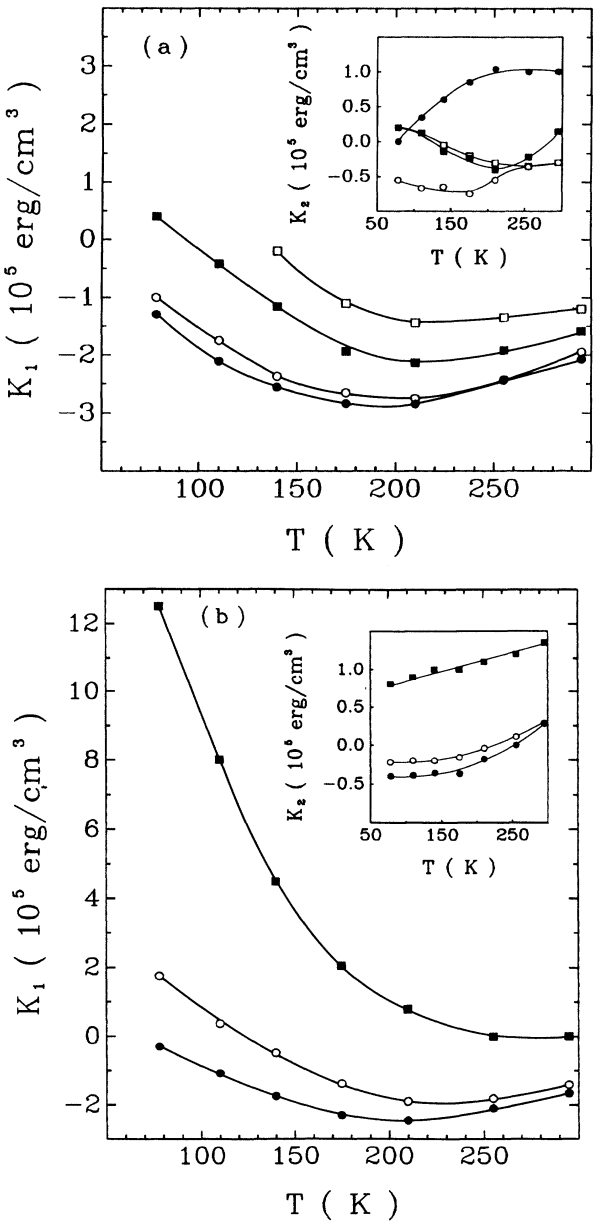

FIG. 7. (a) Temperature dependence of K_1 and K_2 anisotropy parameters for $Fe_{3-x}Ti_xO_4$ series; □ $x=0$, ■ $x=0.05$, ● $x=0.19$, ○ $x=0.28$. (b) Temperature dependence of K_1 and K_2 anisotropy parameters for $Fe_{3-x}Ti_xO_4$ series, ● $x=0.36$, ○ $x=0.41$. ■ $x=0.55$.

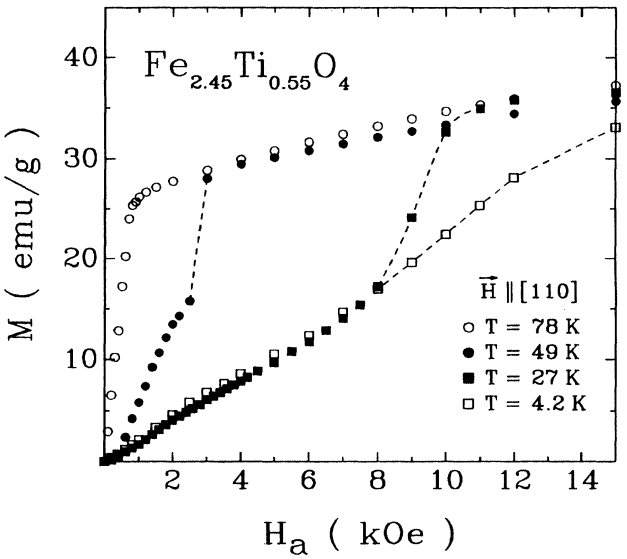

FIG. 8. Magnetization curves of $Fe_{2.45}Ti_{0.55}O_4$ along ⟨110⟩ direction. Axis switching effects are indicated by broken lines.

sign of K_1, and leads to positive values of K_1 at 78 K that are one order of magnitude larger in $Fe_{2.45}Ti_{0.55}O_4$ than in Fe_3O_4. These trends are in agreement with those reported by Syono and Ishikawa[23] for their samples with $x<0.2$; on the other hand, the present effects are smaller than those reported by the same authors[1] at low temperatures for a specimen with $x=0.56$. Comparisons between their results and ours are difficult because of the strong $K_1(x)$ dependence for $x>0.5$ and because of the differences in experimental measurement techniques.

The errors in K_1 and K_2 are estimated to be in the range of ±5% and ±20%, respectively, except at 78 K, where the fit to experimental data was confined to a smaller part of the magnetization curves measured along the medium and hard directions; the available fields of 15 kOe were insufficient to achieve saturation along those directions. This problem was aggravated at lower temperatures and higher Ti concentration, where additional problems of magnetic hysteresis and time-dependent effects complicated the analysis. The time-lag phenomena are interpreted as arising from the slow switching of the lattice distortion at low temperatures when the magnetic field is applied, as is discussed elsewhere in further detail.[6] The axis switching effects encountered here are illustrated in Fig. 8 for the sample with $x=0.55$. The crystal had first been saturated along the [001] direction; measurements were subsequently taken along [110]. The switching phenomena are clearly in evidence. The above effects strongly suggest that there is a significant magnetoelastic contribution to the magnetic anisotropy of samples with high Ti content.

DISCUSSION

When several different types of anisotropy effects combine to produce the magnetic properties of a material it is very difficult to disentangle the individual contributions to the observed magnetization curve. In addition, there are not enough available data in the literature to provide an unambiguous interpretation of the experimental data. We therefore resorted to an interpolation procedure to estimate the magnetoelastic contribution to the magnetic anisotropy, based on published saturation magnetostriction and on elastic constant data.

The subsequent analysis is based on a consideration of several contributions to the total free energy of a system. In ferrites the exchange interactions do not lower the cubic symmetry of the crystal.[24] The elastic stress contributes to the total free energy a term

$$F_{ee}=\tfrac{1}{2}C_{11}(e_{xx}^2+e_{yy}^2+e_{zz}^2)+C_{12}(e_{xx}e_{yy}+e_{yy}e_{zz}+e_{zz}e_{xx}) +\tfrac{1}{2}C_{44}(e_{xy}^2+e_{yz}^2+e_{zx}^2)\ , \tag{9}$$

where C_{11}, C_{12}, and C_{44} are elastic constants and $e_{ij}(i,j=x,y,z)$ are the strain components. There is a further contribution to the total free energy that arises from magnetostrictive stresses, which is the so-called magnetoelastic coupling energy. For cubic crystals this is described by[24]

$$F_{me}=B_1[e_{xx}(\alpha_1^2-\tfrac{1}{3})+e_{yy}(\alpha_2^2-\tfrac{1}{3})+e_{zz}(\alpha_3^2-\tfrac{1}{3})] +B_2[e_{xy}\alpha_1\alpha_2+e_{yz}\alpha_2\alpha_3+e_{zx}\alpha_3\alpha_1]+\cdots\ , \tag{10}$$

where B_1 and B_2 are the magnetoelastic constants.

The equilibrium values e_{ij}^o of e_{ij} are found through minimization of $F=F_{ee}+F_{me}$ with respect to the various e_{ij}. In solving the resulting expressions for e_{ij}^o in terms of the α, B, and C parameters one finds[24]

$$F=K_{me}(\alpha_1^2\alpha_2^2+\alpha_2^2\alpha_3^2+\alpha_3^2\alpha_1^2)-B_1^2/[3(C_{11}-C_{12})]\ , \tag{11}$$

with

$$K_{me}=\frac{B_1^2}{C_{11}-C_{12}}-\frac{B_2^2}{2C_{44}}\ , \tag{12}$$

in which K_{me} represents the magnetoelastic contribution to K_1.

It has been shown[24] that the magnetostrictive constants λ_{100} and λ_{111} in a cubic system may be specified by

$$\lambda_{100}=-\frac{2}{3}\frac{B_1}{C_{11}-C_{12}}\ , \tag{13a}$$

$$\lambda_{111}=-\frac{1}{3}\frac{B_2}{C_{44}}\ . \tag{13b}$$

The above λ values were measured experimentally by Syono and Ishikawa[1] for a titanomagnite specimen with $x=0.56$, which is close to the maximum Ti concentration of $x=0.55$ in the present set of studies. To obtain K_{me} it is unfortunately necessary to determine the elastic constants separately. The only available literature data pertain to magnetite and to US.[25] As stated in the introduction, the Jahn-Teller effect increases with an increasing $(Fe^{2+})_t$ content, and thus comes into prominence near the US composition limit. The attenuation of the elastic constants with increasing Ti content in titanomagnetites was therefore estimated in two ways.

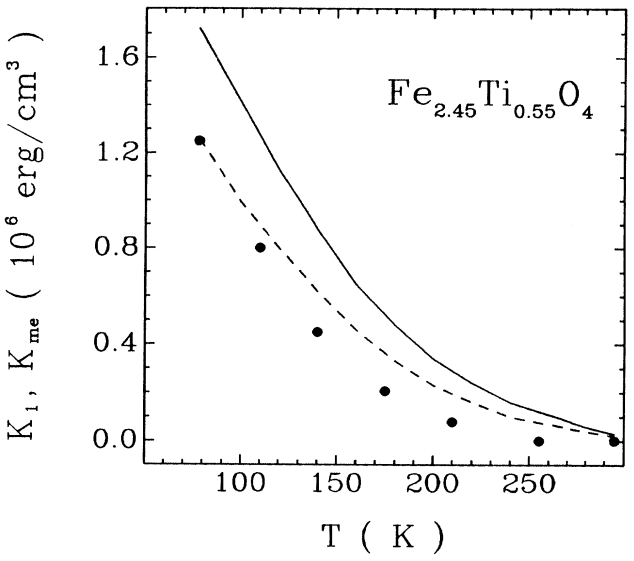

FIG. 9. Temperature dependence of magnetoelastic anisotropy parameter K_{me}. Filled circles: experimental data of K_1 vs T. Solid and broken curves: calculations of K_{me} using models described in text.

Gyorgy *et al.*[9] postulated that the elastic constants due to isolated Jahn-Teller ions at fixed temperature are directly proportional to their concentrations. They based this supposition on measurements of acoustic losses in yttrium iron garnet, which served as indicators of relaxation processes along three equivalent direction of the Jahn-Teller distortion. If this model is adopted the elastic constants are directly proportional to the $(Fe^{2+})_t$ concentration; hence, these constants are expected to vary as $(1.25x-0.25)$ for $x>0.20$. The elastic constants for $x=0.55$, as obtained through the above linear interpolation between Fe_3O_4 and US, were then introduced into Eqs. (12) and (13) to obtain K_{me} as a function of temperature. The calculations are entered in Fig. 9 as the solid curve.

As an alternative we also considered the more sophisticated theory of Kataoka.[11] He successfully rationalized the small elastic constants encountered in US on the basis of an interference between the Jahn-Teller effect arising from the presence of Fe^{2+} on t sites and the spin-lattice interaction of the cations located on o sites. While the mathematical features of the analysis are complex one can show that the key parameter in the analysis is the variable labeled γ_1 which, in first approximation, is given by the ratio m_o/g_o. Here m_o is the coupling constant of the $(Fe^{2+})_o$ ions to the lattice and g_o is the Jahn-Teller coupling constant of the $(Fe^{2+})_t$ ions. From the theory it emerges that $m_o \sim \sqrt{N_o}$ and $g_o \sim \sqrt{N_t}$, where N_o and N_t are the densities of Fe^{2+} cations on the two sites. Thus, in rough approximation, the elastic constants of the TM series should vary as $\sqrt{N_o/N_t} = \sqrt{(1.25-0.25x)/(1.25x-0.25)}$, with $x>0.20$, if the same interference phenomenon applies to members in the TM series. The K_{me} versus T dependence obtained by use of this interpolation scheme for $x=0.55$ is shown as a broken curve in Fig. 9. The experimental data are entered as points.

One should not attach too great a significance to the difference between theory and experiment and to the differences between the two calculated curves. The interpolation procedure is obviously very crude and many factors such as the anisotropy energy associated $(Fe^{2+})_o$ were not considered in the present analysis. The principal point is that the calculated K_{me} for the TM sample $x=0.55$, using either of the above procedures, yields values reasonably close to experiment and that the trend with temperature is correctly reproduced. A more definitive interpretation of the experimental data must await the analysis and publication of actual measurements on the elastic constants on TM specimens with intermediate x values.

CONCLUSIONS

The following conclusions may be drawn.

1. The anisotropy constant K_1 passes through a minimum at $x=0.2$ for the series $Fe_{3-x}Ti_xO_4$, which is independent of temperature. This minimum coincides with the critical composition at which Fe^{2+} first makes its appearance in the tetrahedral interstices, as shown in Fig. 1. Unfortunately, it was not possible to determine K_1 for the composition range $x>0.6$ because of interference by hysteretic phenomena, especially at low temperatures.

2. In the composition range $x>0.2$ at low temperatures, K_1 and the anisotropy, as well as the magnetostriction, become very large with further increases in x. These findings render it likely that the above changes all have their origin in the presence of Fe^{2+} on tetrahedral sites and that they are associated with the concomitant Jahn-Teller effect.

3. The magnetoelastic contribution to the anisotropy energy was estimated as discussed earlier. We found that this contribution dominated the total magnetic anisotropy, independent of the model that was chosen to analyze this effect. Both the isolated ion model or the interference effect between the Jahn-Teller distortion and the octahedral spin-lattice coupling were considered. Within the rather sizable theoretical uncertainties the experimental variation of K_1 with temperature was satisfactorily reproduced.

ACKNOWLEDGMENTS

This research was supported by Grants Nos. NSF DMR 86 16533 AO2 and DMR 89 21293. One of us (J.S.) gratefully acknowledges support from the NSF Grant No. DMR-89-05605, as well as partial support from Ohio Northern University. We wish to thank Professor R. Argaón and P. Metcalf for their assistance in supplying some of the samples.

*Permanent address: AGH Technical University, PL-30-059 Kraków, Poland.

[1]Y. Syono and Y. Ishikawa, J. Phys. Soc. Jpn. **19**, 1752 (1964).
[2]S. K. Banerjee, W. O'Reilly, T. C. Gibb, and N. N. Greenwood, J. Phys. Chem. Solids **28**, 1323 (1967).
[3]E. Schmidbauer and P. W. Readman, J. Magn. Magn. Mat. **27**, 114 (1982).
[4]Z. Kąkol, J. Sabol, and J. M. Honig, Phys. Rev. B **43**, 649 (1991).
[5]Y. Ishikawa, S. Sato, and Y. Syono, J. Phys. Soc. Jpn. **31**, 452 (1971).
[6]Y. Ishikawa and Y. Syono, J. Phys. Soc. Jpn. **31**, 461 (1971).
[7]Y. Syono, Y. Fukai, and Y. Ishikawa, J. Phys. Soc. Jpn. **31**, 471 (1971).
[8]Y. Ishikawa and Y. Syono, Phys. Rev. Lett. **26**, 133 (1971).
[9]E. M. Gyorgy, R. C. Le Craw, and M. D. Sturge, J. Appl. Phys. **37**, 1303 (1966).
[10]M. Kataoka and J. Kanamori, J. Phys. Soc. Jpn. **32**, 113 (1972).
[11]M. Kataoka, J. Phys. Soc. Jpn. **36**, 456 (1974).
[12]S. Akimoto, T. Katsura, and M. J. Yoshida, J. Geomagn. Geoelect. **9**, 165 (1957).
[13]L. Néel, Adv. Phys. **4**, 191 (1955).
[14]R. Chevallier, J. Bolfa, and S. Mathieu, Bull. Soc. Fr. Minéral. Cristallogr. **78**, 307 (1955).
[15]W. O'Reilly and S. K. Banerjee, Phys. Lett. **17**, 237 (1965).
[16]G.Blasse, Philips Res. Rep. Suppl. No. 3 (1964).
[17]Z. Kąkol, J. Sabol, and J. M. Honig, J. Appl. Phys. **69**, 4822 (1991).
[18]H. R. Harrison and R. Aragón, Mater. Res. Bull. **13**, 1097 (1978).
[19]R. Aragón, D. J. Buttrey, J. P. Shepherd, and J. M. Honig, Phys. Rev. B **31**, 430 (1985).
[20]R. Aragón and R. H. McCallister, Phys. Chem. Minerals **8**, 112 (1982).
[21]J. M. Honig and R. Aragón, Z. Anorg. Allg. Chem. **540/541**, 80 (1986).
[22]Z. Kąkol and J. M. Honig, Phys. Rev. B **40**, 9090 (1989).
[23]Y. Syono and Y. Ishikawa, J. Phys. Soc. Jpn. **18**, 1230 (1963).
[24]J. Kanamori, *Magnetism,* edited by G. T. Rado and H. Suhl (Academic, New York, 1963), Vol. **1**, 127.
[25]F. Birch, *Handbook of Physical Constants,* edited by S. P. Clark Jr. (Geol. Soc. Amer. Memoir, Washington, 1966), Vol. 97, p. 87.